Columbia University
in the City of New York

DEPARTMENT OF CIVIL ENGINEERING
AND ENGINEERING MECHANICS

MONTE CARLO SOLUTION OF STRUCTURAL DYNAMICS

by

M. Shinozuka

19990722 058

March 1972

Technical Report No. 19

Prepared for

The National Science Foundation

An Invited Paper

at the

National Symposium on Computerized

Structural Analysis and Design

to be held at the

George Washington University, Washington, D. C.

March 27 - 29, 1972

1. Introduction

In the last two decades, much research effort has been devoted to the application of the stochastic process theory in the general area of engineering mechanics and structural engineering for the purpose of predicting the dynamic structural performance with a better accuracy and of assessing the over-all structural safety with a better reliability by considering more realistic analytical models of load-structure systems.

Naming only a few, possible applications of this stochastic approach include (a) analysis of panel vibrations of aircraft and submarines induced by boundary layer turbulence, (b) analysis of ship oscillations caused by ocean waves, particularly during a storm, (c) analysis of aircraft response to gust vertical velocity, (d) response analysis of off-shore structures to wave and wind forces, (e) statistical strength analysis of engineering materials, particularly of modern composite materials, with randomly distributed thermo-mechanical properties, (f) analysis of the effect of randomness in geometrical configuration of and mechanical constraint on a structural component due, for example, to fabrication errors on the vibration and buckling eigenvalues and, (g) study of random surface roughness of bridge pavement and airport run-way for the purposes of analyzing the vehicle and aircraft vibration caused by the roughness and of stress analysis

of pavement systems under the action of vehicles and aircraft.

In spite of the recent remarkable advance in this area of study, however, the present state of art still leaves a number of difficulties unsolved that must be overcome before the approach becomes more useful. Such problem areas include

(1) random response analysis of highly nonlinear structures,

(2) failure analysis of structures under random loading,

(3) analysis of extremely complex systems and,

(4) random eigenvalue problems.

The recent advent of high speed digital computers, however, has made it not only possible but also highly practical to apply the Monte Carlo techniques to a large variety of engineering problems. The present paper presents a technique of digital simulation of multivariate and/or multidimensional Gaussian random processes (homogeneous or nonhomogeneous) which can represent physical processes germane to structural engineering. The paper also describes a method of digital simulation of envelope functions. Such simulations are accomplished in terms of a sum of cosine functions with random phase angles and used as the basic tool in a general Monte Carlo method of solution to a wide class of problems in structural engineering, particularly those mentioned above.

2. Simulation of a Random Process: A Background

A basic representation of a homogeneous Gaussian (one-dimensional and one-variate) random process $f_0(x)$ with mean zero and spectral density $S_0(\omega)$ in the form of the sum of the cosine functions has existed for some time [1];

$$f(x) = \sqrt{2} \sum_{k=1}^{N} A_k \cos(\omega_k x - \Phi_k) \tag{1}$$

where Φ_k are random angles distributed uniformly between 0 and 2π and independent of Φ_j $(k \neq j)$, and

$$A_k = [S_1^0(\omega_k) \Delta\omega]^{\frac{1}{2}} , \quad \omega_k = (k - \tfrac{1}{2}) \Delta\omega \tag{2}$$

with

$$S_1^0(\omega) = 2S_0(\omega) \tag{3}$$

being the one-sided spectral density function (see Fig. 1). For digital simulation of a simple function $\bar{f}(x)$ of $f(x)$ and therefore of $f_0(x)$, Eq. 1 is used with Φ_k being replaced by their realized values φ_k;

$$\bar{f}(x) = \sqrt{2} \sum_{k=1}^{N} A_k \cos(\omega_k x - \varphi_k) \tag{4}$$

With the aid of Eqs. 1 and 4, it is easy to show that Eq. 1 is ergodic at least up to the second moment.

Speaking of structure-related applications, however, until Borgman [2] published a paper simulating ocean surface elevation

as a multidimensional process essentially in the same form, little

attention had been paid to this representation in spite of its

substantial advantage over the standard method in which a random

process was digitally generated as output of an appropriate

(analytical) filter subjected to a simulated white process. The

use of this filtering technique, although limited in its practical

applications to a one-variate one-dimensional process has dominated

a large number of papers involving simulations of a random

process.

Practical digital simulation of a multidimensional process

has been made possible, as mentioned above, by Borgman [2] in

principle through the preceding expression consisting of a sum

of cosines and by Shinozuka [3] whose method reduces, in case of

one-variate one-dimensional situations to the use of the following

expression;

$$f(x) = \sigma \left(\frac{2}{N}\right)^{\frac{1}{2}} \sum_{k=1}^{N} \cos(\omega_k x - \varphi_k) \tag{5}$$

where φ_k are as previously defined and ω_k are realized values

of random frequencies distributed according to the density

function $g(\omega) = S_o(\omega)/\sigma^2$ with

$$\sigma^2 = \int_{-\infty}^{\infty} S_o(\omega) \, d\omega \tag{6}$$

Borgman [2] and Shinozuka [3] also investigated the digital

simulation of the multivariate (but one-dimensional) process,

4

the former making use of the filtering technique and the latter

in the more convenient form of the sum of the cosine functions.

Reference [4] shows that the autocorrelation function

$R(\xi)$ of $f(x)$ converges to $R_0(\xi)$ of $f_0(x)$ in the form of $1/N^2$

as $N \to \infty$. The same trend in convergence can be shown [4] to

exist between the spectral element $S(\omega) \Delta\omega$ of $f(x)$ and $S_0(\omega) \Delta\omega$

of $f_0(x)$.

It is interesting to note that $f(x)$ in Eq. 1 can be

interpreted as a canonical expansion of a Gaussian process $f_0(x)$

with mean zero and spectral density $S_0(\omega)$. To see this, express

$f_0(x)$ in the form of the spectral representation

$$f_0(x) = \int_{-\infty}^{\infty} e^{i\omega x} dZ(\omega) \tag{7}$$

where $Z(\omega)$, called spectral process, is orthogonal in the sense

that the increments $dZ(\omega_1)$ and $dZ(\omega_2)$ are uncorrelated when

$\omega_1 \neq \omega_2$.

Employing the orthogonal condition of $Z(\omega)$, the auto-

correlation function of $f_0(x)$ is found to be

$$R_0(\xi) = E[f_0(x) f_0(x+\xi)] = \int_{-\infty}^{\infty} e^{i\omega\xi} E|dZ(\omega)|^2 \tag{8}$$

where E indicates the expected value.

Assume that the spectral density function $S_0(\omega)$ exists.

Then $E|dZ(\omega)|^2 = S_0(\omega) d\omega$, and Eq. 8 is reduced to the well-

known Wiener-Khintchine relationship. For the case when $f_0(x)$

is real, Eq. 7 becomes [4]

$$f_o(x) = \int_o^\infty [\cos \omega x dU(\omega) + \sin \omega x dV(\omega)] \qquad (9)$$

where $U(\omega)$ and $V(\omega)$ for any $\omega \geq 0$ are two mutually orthogonal

processes, both real and with orthogonal increments, such that

$$E[dU(\omega)]^2 = E[dV(\omega)]^2 = S_1^o(\omega) \, d\omega$$

It is pointed out that if one defines

$$dU(\omega_k) = [2S_1^o(\omega_k) \, \Delta\omega]^{\frac{1}{2}} \cos \Phi_k = \sqrt{2} \, A_k \cos \Phi_k$$

$$\qquad (10)$$

$$dV(\omega_k) = [2S_1^o(\omega_k) \, \Delta\omega]^{\frac{1}{2}} \sin \Phi_k = \sqrt{2} \, A_k \sin \Phi_k$$

where ω_k, $\Delta\omega$ and Φ_k are defined in Eqs. 1 and 2, then all the

conditions imposed on $U(\omega)$ and $V(\omega)$ are satisfied, and Eq. 1

is basically consistent with the spectral representation.

It is seen from Eq. 9 that a homogeneous process is addi-

tively built up by orthogonal oscillations with random amplitudes.

A canonical expression of a real random process $f_o(x)$

can be written in the form [5];

$$f_o(x) = \sum_{k=1}^\infty \alpha_k v_k(x) \qquad (11)$$

where α_k are uncorrelated random variables with mean zero and

$v_k(x)$ are real (deterministic) functions of x; α_k are called

the coefficients of the canonical expansion and $v_k(x)$ the

coordinate functions.

By multiplying both sides of Eq. 11 by α_j, taking the expected values and using the fact that α_j are uncorrelated, one can show that

$$v_j(x) = \frac{1}{D_j} E[\alpha_j f_0(x)]$$ (12)

where D_j is the variance of α_j;

$$D_j = E[\alpha_j^2]$$ (13)

At this point, write $f_0(x)$ in Eq. 9 in the following approximate form;

$$f(x) = \sum_{k=1}^{N} [\cos \omega_k x \, dU(\omega_k) + \sin \omega_k x \, dV(\omega_k)]$$

$$= \sqrt{2} \sum_{k=1}^{N} (A_k \cos \omega_k x \cos \Phi_k + A_k \sin \omega_k x \sin \Phi_k)$$

$$= \sqrt{2} \sum_{k=1}^{N} A_k \cos(\omega_k x - \Phi_k)$$ (14)

This is an approximation to $f_0(x)$ since the integration is replaced by a summation involving a finite number (N) of terms. The degree of the approximation depends on (a) whether the cut-off frequency ω_u (see Fig. 1) is large enough and (b) whether $\Delta\omega$ in Eq. 2 is small enough so that

$$A_k^2 = \int_{(k-1)\Delta\omega}^{k\Delta\omega} S_1^0(\omega) \, d\omega \doteq S_1^0(\omega_k) \, \Delta\omega$$ (15)

is valid. Being the sample function of $f(x)$, $\bar{f}(x)$ possesses the same approximate nature when considered as the sample function of $f_0(x)$.

Within the context of this approximation, Eq. 14 can be interpreted as an (truncated) canonical expansion of $f_0(x)$ in the form of Eq. 11 if α_j and $v_j(x)$ are defined as

$$\alpha_{2j-1} = \sqrt{2}\,A_j \cos \phi_j, \qquad v_{2j-1}(x) = \cos \omega_j x$$

$$(j=1,2,\ldots,N) \quad (16)$$

$$\alpha_{2j} = \sqrt{2}\,A_j \sin \phi_j, \qquad v_{2j}(x) = \sin \omega_j x$$

In fact, the coordinate functions in Eq. 16 follow from Eq. 12 if the coefficients α_k in Eq. 16 and $f(x)$ in the form of Eq. 14 are used therein.

It can then be shown [5] (again within the context of the approximation mentioned above) that if these $v_k(x)$ defined in Eq. 16 are used, then for any given number of N and for the particular selection of α_k in Eq. 16, Eq. 14 gives the best approximation to the random function $f_0(x)$ in the sense that, among all possible series expansion of $f_0(x)$ having the same number of terms, Eq. 14 minimizes the expectation of the square of the residual term at any value of x.

There is another constraint to be imposed upon $\Delta\omega$. This constraint is due to the periodicity of the sample function $\bar{f}(x)$.

Obviously, the period of $\bar{f}(x)$ is $T_0 = 2\pi/\Delta\omega$ and therefore, depending on the purpose of the simulation, $\Delta\omega$ has to be so chosen that T_0 is long enough for that purpose.

A significant improvement in the efficiency of digital simulation has recently been suggested by Yang [6] writing

$$\bar{f}(x) = \sqrt{\Delta\omega} \quad \text{Re } F(x) \tag{17}$$

in which Re $F(x)$ represents the real part of $F(x)$ and

$$F(x) = \sum_{k=1}^{N} \left\{ [2 S_1^o(\omega_k)]^{\frac{1}{2}} e^{-i\varphi_k} \right\} e^{i\omega_k t} \tag{18}$$

is the finite complex Fourier transform of $[2S_1^o(\omega_k)]^{\frac{1}{2}} e^{-i\varphi_k}$ with ω_k and φ_k defined in Eqs. 1 and 2. The advantage of Eq. 18 is such that the function $F(x)$ can readily be computed by applying the fast Fourier transform (FFT) algorithm, hence avoiding the time-consuming computation of a large number of cosine functions.

In the preceding discussion, the spacing $\Delta\omega$ in the frequency domain has been taken as constant. This, however, does not necessarily have to be always observed. It is possible and in fact may even be advisable to use variable spacings depending on the extent of fluctuation of the spectral density to optimize the number of cosine terms in the summation in Eq. 1; finer spacings in those domains of frequency where the fluctuation of the spectral density is more rapid and coarser spacings elsewhere.

It is also likely that such variable spacings will increase the period T_0 of the simulated process. If this is done, however, the simulation through the FFT technique does not appear to be possible.

In the same reference [6], Yang also proposed to simulate the envelope process $V_0(t)$ of a random process $f_0(x)$ by following the definition of the envelope process [7]

$$V_0(t) = [f_0^2(x) + \hat{f}_0^2(x)]^{\frac{1}{2}} \qquad (19)$$

where $\hat{f}_0(x)$ is the Hilbert transform of $f_0(x)$ and, in the present case, can be written as

$$\hat{f}_0(x) = \int_0^\infty [\sin \omega t \, dV(\omega) - \cos \omega t \, dV(\omega)] \qquad (20)$$

It then follows that $\hat{f}_0(x)$ can be simulated as $\hat{f}(x)$;

$$\hat{f}(x) = \sqrt{2} \sum_{k=1}^{N} A_k \sin(\omega_k x - \varphi_k) \qquad (21)$$

Hence, the envelope process $V_0(t)$ can be simulated as $V(t)$;

$$V(t) = [f^2(x) + \hat{f}^2(x)]^{\frac{1}{2}} \qquad (22)$$

As an example, consider the response process $y_0(t)$ of single degree of freedom system to a Gaussian white noise excitation $x_0(t)$ with the constant spectral density S_0;

$$\ddot{y}_0(t) + 2\zeta\omega_0 \dot{y}_0(t) + \omega_0^2 y_0(t) = x_0(t) \qquad (23)$$

It is well known that the spectral density of $y_0(t)$ is

$$S_y(\omega) = \frac{S_0}{(\omega^2 - \omega_0^2)^2 + 4\zeta^2\omega_0^2\omega^2} \qquad (24)$$

and the standard deviation σ_y of $y_0(t)$ is

$$\sigma_y = \left(\frac{\pi S_0}{2 \zeta \omega_0^3} \right)^{\frac{1}{2}} \qquad (25)$$

With the aid of Eqs. 1, 21 and 22, a segment of sample function $\bar{y}(t)$ of simulated process $y(t)$ for $y_0(t)$ and that of simulation $V(t)$ of the envelope process $V_0(t)$ are computed and shown in Fig. 2 and 3. Fig. 2 is for the case where the damping coefficient $\zeta = 0.02$ and hence the process $y_0(t)$ is narrow-band. This fact is well demonstrated by the smooth behavior of the sample envelope. When the local maxima of the sample envelope do not coincide with the local maxima (peaks) of the process, they reflect the local minima (troughs) of the simulated process. Fig. 3 shows the sample functions of $V(t)$ and $y(t)$ for $\zeta = 0.5$. In this case, the process $y_0(t)$ is substantially wide-band and this fact is clearly seen from the much wilder fluctuation of both simulated envelope and simulated process, although the simulated envelope surprisingly well reflects peaks and troughs of the simulated process even though the process $y_0(t)$ is wide-band. In terms of simulation efficiency, the computer time will be significantly reduced if one is interested in peak- and trough-values of the process and if the process is narrow-band, since then the smooth nature of the envelope function makes it possible to use much larger interval between successive time instants at which the values of

11

the simulated process is evaluated. The order of magnitude of

this interval can be that of the apparent period of the process,

which obviously is much too large for simulation of the process

itself.

Again following Yang [6], write $\hat{f}(t)$ as

$$\hat{f}(t) = \sqrt{\Delta\omega}\ \text{Im}\, F(t) \tag{26}$$

and hence $V(t)$ can also be simulated through the FFT technique.

It appears at this time that the method of simulation

considered herein (Eq. 1) has a difficulty in achieving a

reliable evaluation of the first passage time distribution

when the threshold value is much larger than the standard de-

viation of the process. Lyon's work [8] points to this fact,

although this difficulty is by no means unique to the proposed

method. It is suggested, however, that a further investigation

be performed on this point.

The Gaussian property of the simulated process (Eq. 1)

comes from the central limit theorem because it consists of a

sum of a large number of independent functions of time (see

pp. 182 - 183 in [1]). Efficient simulation, or straight forward

simulation if not efficient, of a non-Gaussian process appears

to be an open problem at this time unless the process is restricted

to a certain class of processes such as the filtered Poisson

process.

In the following sections, a method for digital simulation

of multidimensional and/or multivariate processes are briefly

described. However, for these cases, the rigorous discussions on the interpretation as canonical expansion, the use of the FFT technique in actual digital computation, the envelope simulation, the problem of the first excursion time, the simulation of non-Gaussian processes, the convergence of the auto-correlation function and the spectral density of the simulated process to the respective target values, etc., are mostly subjects of future studies.

3. Simulation of a Multidimensional Homogeneous Process

The autocorrelation function of an n-dimensional homogeneous real process $f_o(\underline{x})$ defined by

$$R_o(\underline{\xi}) = E[f_o(\underline{x}_1) f_o(\underline{x}_2)]$$

is even in $\underline{\xi}$ (symmetric with respect to the origin of the n-dimensional space)

$$R_o(\underline{\xi}) = R_o(-\underline{\xi}) \tag{27}$$

where $\underline{x}_1$ and $\underline{x}_2$ are space vectors and $\underline{\xi} = \underline{x}_2 - \underline{x}_1$ is the separation vector. Assume that the n-fold Fourier transform of $R_o(\underline{\xi})$ exists. The spectral density function of $f_o(\underline{x})$ is then defined as

$$S_o(\underline{\omega}) = \frac{1}{(2\pi)^n} \int_{-\infty}^{\infty} R_o(\underline{\xi}) \, e^{-i\underline{\omega} \cdot \underline{\xi}} d\underline{\xi} \tag{28}$$

where $\underline{\omega}$ is the frequency (wave number) vector and $\underline{\omega} \cdot \underline{\xi}$ is the inner product of $\underline{\omega}$ and $\underline{\xi}$, and, for simplicity

$$\int_{-\infty}^{\infty} (\ ) \, d\underline{\xi} \equiv \int_{-\infty}^{\infty} \overset{\text{n-fold}}{\cdots\cdots\cdots} \int_{-\infty}^{\infty} (\ ) \, d\xi_1 d\xi_2 \ldots d\xi_n$$

with n being the dimension of the vector $\underline{\xi}$. It follows from Eq. 27 that

$$\int_{-\infty}^{\infty} R_o(\underline{\xi}) \sin(\underline{\omega} \cdot \underline{\xi}) \, d\underline{\xi} = 0$$

and, therefore, from Eq. 28

$$S_o(\underline{\omega}) = S_o(-\underline{\omega}) \tag{29}$$

14

Then

$$S_o(\underline{\omega}) = \frac{1}{(2\pi)^n} \int_{-\infty}^{\infty} R_o(\underline{\xi}) \cos(\underline{\omega} \cdot \underline{\xi}) \, d\underline{\xi} \qquad (30)$$

and is real.

It can be shown [9] that $R_o(\underline{\xi})$ is nonnegative definite and therefore it has a nonnegative n-fold Fourier transform;

$$S_o(\underline{\omega}) \geq 0 \qquad (31)$$

Based on these properties of $S_o(\underline{\omega})$, a method of simulating $f_o(\underline{x})$ is proposed in the following:

Consider an n-dimensional homogeneous process with mean zero and spectral density function $S_o(\underline{\omega})$ which is of insignificant magnitude outside the region defined by

$$-\infty < \underline{\omega}_\ell \lessapprox \underline{\omega} \leq \underline{\omega}_u < \infty$$

and denote the interval vector by

$$(\Delta\omega_1, \Delta\omega_2, \ldots, \Delta\omega_n) = \left(\frac{\omega_{1u} - \omega_{1\ell}}{N_1}, \frac{\omega_{2u} - \omega_{2\ell}}{N_2}, \ldots, \frac{\omega_{nu} - \omega_{n\ell}}{N_n} \right) \quad (32)$$

where usually $\underline{\omega}_\ell = -\underline{\omega}_u$. Then the process can be simulated by the series

$$f(\underline{x}) = \sqrt{2} \sum_{k_1=1}^{N_1} \sum_{k_2=1}^{N_2} \ldots \sum_{k_n=1}^{N_n} [S_o(\omega_{1k_1}, \omega_{2k_2}, \ldots, \omega_{nk_n}) \Delta\omega_1 \Delta\omega_2 \ldots \Delta\omega_n]^{\frac{1}{2}}$$

$$\cdot \cos(\omega_{1k_1} x_1 + \omega_{2k_2} x_2 + \ldots \omega_{nk_n} x_n + \Phi_{k_1 k_2 \ldots k_n}) \qquad (33)$$

where

$$\Phi_{k_1 k_2 \ldots k_n} = \text{independent random phase uniformly}$$

$$\text{distributed between } 0 \text{ and } 2\pi$$

$$\omega_{ik_i} = \omega_{i\ell} + (k_i - \tfrac{1}{2}) \Delta\omega_i \qquad k_i = 1, 2, \ldots, N_i \qquad i = 1, 2, \ldots, n$$

As in the one-dimensional case, the digital simulation $\bar{f}(\underline{x})$ of $f(\underline{x})$ can be achieved by using Eq. 33 with $\Phi_{k_1 k_2 \ldots k_n}$ being replaced by their realized values $\varphi_{k_1 k_2 \ldots k_n}$.

To avoid the lengthy expressions in the subsequent discussion, $\bar{f}(\underline{x})$ will be written in the following compact form:

$$\bar{f}(\underline{x}) = \sqrt{2} \sum_{k=1}^{N} A(\underline{\omega}_k) \cos(\underline{\omega}_k \cdot \underline{x} + \varphi_k) \tag{34}$$

where

$$N = N_1 N_2 \ldots N_n$$

$$A(\underline{\omega}_k) = [S_o(\underline{\omega}_k) \Delta\omega_1 \Delta\omega_2 \ldots \Delta\omega_n]^{\frac{1}{2}} = [S_o(\underline{\omega}_k) \Delta\underline{\omega}]^{\frac{1}{2}} \tag{35}$$

It is noted that if the symmetric condition of $S_o(\underline{\omega})$ is used, N in Eq. 33 can be reduced by one-half. Furthermore, if the process is isotropic, N is reduced to $\dfrac{N}{2^n}$. Fig. 4 illustrates the significance of $A(\underline{\omega}_k)$ for two-dimensional cases where, however, $A_{k_1 k_2}$ is written for $A(\omega_{1k_2}, \omega_{2k_2})$.

It can be shown [4] that the ensemble average of $f(\underline{x})$ is zero, and the autocorrelation function $R(\underline{\xi})$ of $f(\underline{x})$, becomes

$$R(\underline{\xi}) = \sum_{k=1}^{N} A^2(\underline{\omega}_k) \cos(\underline{\omega}_k \cdot \underline{\xi}) \tag{36}$$

Upon substituting $A^2(\underline{\omega}_k) = S_o(\underline{\omega}_k) \Delta\omega$, and taking the limit as $N \to \infty$ (in the sense that $N_1, N_2, \ldots, N_n \to \infty$ simultaneously) one obtains

$$R(\underline{\xi}) = \int_{-\infty}^{\infty} S_o(\underline{\omega}) \cos(\underline{\omega} \cdot \underline{\xi}) \, d\underline{\omega} = R_o(\underline{\xi}) \qquad (37)$$

where it is assumed $S_o(\underline{\omega}) = 0$ for $\underline{\omega} < \underline{\omega}_\ell$ and $\underline{\omega} > \underline{\omega}_u$.

This indicates that, when the ensemble average is considered, the simulated process $f(\underline{x})$ possesses the target autocorrelation $R_o(\underline{\xi})$ and therefore the target spectral density $S_o(\underline{\omega})$.

It can also be shown [4] that the temporal (or spatial) mean $< f(\underline{x}) >$ is zero and the temporal autocorrelation $R^*(\underline{\xi}) = < f(\underline{x}) \, f(\underline{x} + \underline{\xi}) >$ becomes

$$R^*(\underline{\xi}) = \sum_{k=1}^{N} A^2(\underline{\omega}_k) \cos(\underline{\omega}_k \cdot \underline{\xi}) \qquad (38)$$

As $N \to \infty$, Eq. 38 becomes

$$R^*(\underline{\xi}) = \int_{-\infty}^{\infty} S_o(\underline{\omega}) \cos(\underline{\omega} \cdot \underline{\xi}) \, d\underline{\omega} = R_o(\underline{\xi}) \qquad (39)$$

From Eqs. 36 and 38, it is seen that the process $f(\underline{x})$ in Eq. 33 is ergodic regardless of the size of N. This makes the method directly applicable to a time domain analysis in which the ensemble average can be evaluated in terms of the temporal average.

Note that the simulated process is Gaussian by virtue of the central limit theorem.

As an example of digital simulation of a multidimensional process, consider a two-dimensional homogeneous Gaussian process $f_o(t,x)$ with mean zero and spectral density

$$S_o(\omega,k) = \frac{KL^2}{2\pi^2} \cdot \frac{|\omega|}{(1+c^2\omega^2)^{4/3}} \cdot \frac{\alpha|\omega|}{\pi(\alpha^2\omega^2+k^2)} \qquad (40)$$

where t and x represent the time and the distance respectively and, correspondingly, ω and k the frequency and the wave number. It is known that such process $f_o(t,x)$ is a satisfactory model of a fluctuating part of wind velocity along a straight line direction x. In the wind study, however, it is customary to consider the Fourier transform $S_o(\omega,\xi)$ of the autocorrelation $R_o(\tau,\xi) = E[f_o(t,x) \, f_o(t+\tau, x+\xi)]$ only with respect to τ. In fact, the form of $S_o(\omega,\xi)$ consistent with Eq. 40 is

$$S_o(\omega,\xi) = \frac{KL^2}{2\pi^2} \cdot \frac{|\omega|}{(1+c^2\omega^2)^{4/3}} \cdot e^{-\alpha|\omega||\xi|} \qquad (41)$$

a familiar form for a fluctuating part of wind velocity at the reference altitude of 33 feet where $L = 4000$ ft., $K = $ surface drag coefficient, $\alpha = $ constant, $C = L/(2\pi U_{33})$ with U_{33} being the mean wind velocity at the reference altitude. For $U_{33} = 40$ mph, $\alpha = 0.02$ ft $\cdot$ sec and $K = 0.03$, the sample functions $\bar{f}(t,\xi)$ of $f_o(t,\xi)$ are computed and shown in Fig. 5 at $\xi = 0$, 50 and 200 ft. One can easily see in this example that the correlation almost disappears as the separation ξ increases to 200 ft.

Consider a set of m homogeneous Gaussian n-dimensional processes $f_j^o(\underline{x})$ $(j = 1, 2, \ldots \ldots m)$ with mean zero and with the cross-spectral density matrix $S(\omega)$ defined by

$$
\begin{bmatrix}
S_{11}^o(\underline{\omega}) & S_{12}^o(\underline{\omega}) & \cdots & S_{1m}^o(\underline{\omega}) \\
S_{21}^o(\underline{\omega}) & S_{22}^o(\underline{\omega}) & \cdots & S_{2m}^o(\underline{\omega}) \\
\cdots\cdots\cdots\cdots\cdots\cdots\cdots\cdots\cdots \\
S_{m1}^o(\underline{\omega}) & S_{m2}^o(\underline{\omega}) & \cdots & S_{mm}^o(\underline{\omega})
\end{bmatrix}
\tag{42}
$$

where $S_{jk}^o(\underline{\omega})$ is the n-fold Fourier transform of the cross correlation $R_{jk}^o(\underline{\xi})$.

Due to the fact that $R_{jk}^o(\underline{\xi}) = R_{kj}^o(-\underline{\xi})$, one obtains

$$
S_{jk}^o(\underline{\omega}) = \bar{S}_{kj}^o(\underline{\omega})
\tag{43}
$$

where the bar indicates the complex conjugate.

The matrix $S^o(\underline{\omega})$ is therefore Hermitian. As in the case of a one-dimensional multivariate process [10], it can be shown [4] that the matrix $S^o(\underline{\omega})$ is also nonnegative definite.

Suppose one can find a matrix $H(\underline{\omega})$ which possesses n-dimensional Fourier transform and satisfies the equation

$$
S^o(\underline{\omega}) = H(\underline{\omega}) \, \bar{H}(\underline{\omega})^T
\tag{44}
$$

where $S^o(\underline{\omega})$ is the specified target cross-spectral matrix and T indicate the transpose. Then $f_j(\underline{x})$ $(j=1, 2, \ldots, m)$ can be

simulated by the following filtering technique [2, 11];

$$f_j(\underline{x}) = \sum_{k=1}^{m} \int_{-\infty}^{\underline{x}} h_{jk}(\underline{x} - \underline{\xi}) \, \eta_k(\underline{\xi}) d\underline{\xi} \tag{45}$$

where $h_{jk}(\underline{x})$ is the n-dimensional Fourier transofrm of $H_{jk}(\underline{\omega})$;

$$h_{jk}(\underline{x}) = \int_{-\infty}^{\infty} H_{jk}(\underline{\omega}) e^{-i\underline{\omega} \cdot \underline{x}} d\underline{\omega}$$

and $\eta_k(\underline{x})$ is an independent n-dimensional normalized white

noise component such that

$$E[\eta_j(\underline{x}_1)\eta_k(\underline{x}_2)] = \delta(\underline{x}_1 - \underline{x}_2)\delta_{jk}$$

with

$$\delta(\underline{x}_1 - \underline{x}_2) = \delta(x_{11} - x_{21})\delta(x_{12} - x_{22}) \ldots \ldots \delta(x_{1n} - x_{2n})$$

It can be easily verified that the $f_j(\underline{x})$ $(j = 1, \ldots m)$,

as simulated by Eq. 45, satisfy Eq. 44 and thus represent the

target processes.

To find the matrix $H(\underline{\omega})$ in an efficient way, one can

assume that $H(\underline{\omega})$ is a lower triangular matrix;

$$H(\underline{\omega}) = \begin{bmatrix} H_{11}(\underline{\omega}) & 0 & 0 & \ldots & 0 \\ H_{21}(\underline{\omega}) & H_{22}(\underline{\omega}) & \cdot & \ldots & 0 \\ \ldots\ldots\ldots\ldots\ldots\ldots\ldots\ldots\ldots\ldots\ldots \\ H_{m1}(\underline{\omega}) & H_{m2}(\underline{\omega}) & \cdot & \ldots & H_{mm}(\underline{\omega}) \end{bmatrix}$$

Substituting above into Eq. 44, solutions are obtained (see

Ref. 12 for similar derivation) as

$$H_{kk}(\omega) = \left[\frac{D_k(\omega)}{D_{k-1}(\omega)}\right]^{\frac{1}{2}} \qquad k = 1, 2, \ldots m \qquad (46)$$

where $D_k(\omega)$ is the k-th principal minor of $S^o(\omega)$ with D_o being defined as unity, and

$$H_{jk}(\omega) = H_{kk}(\omega) \frac{S^o\binom{1,2,\ldots,k-1,j}{1,2,\ldots,k-1,k}}{D_k(\omega)} \qquad \begin{array}{l} k = 1, 2, \ldots m \\[4pt] j = k+1, \ldots m \end{array} \qquad (47)$$

where

$$S^o\binom{1,2,\ldots k-1,j}{1,2,\ldots k-1,k} = \begin{vmatrix} S^o_{11} & S^o_{12} & \cdots & S^o_{1,k-1} & S^o_{1k} \\[4pt] S^o_{21} & S^o_{22} & \cdots & S^o_{2,k-1} & S^o_{2k} \\[4pt] \cdots & \cdots & \cdots & \cdots & \cdots \\[4pt] S^o_{k-1,1} & S^o_{k-1,2} & \cdots & S^o_{k-1,k-1} & S^o_{k-1,k} \\[4pt] S^o_{j1} & S^o_{j2} & \cdots & S^o_{j,k-1} & S^o_{jk} \end{vmatrix}$$

is the determinant of a submatrix obtained by deleting all elements except the $(1,2,\ldots k-1,j)$-th row and $(1,2,\ldots k-1,k)$-th column of $S^o(\omega)$.

It is noted that the above decomposition is valid only when the matrix $S^o(\omega)$ is hermitian and positive definite as can be seen from Eq. 46.

Because the cross-spectral density matrix $S^o(\omega)$ is known to be only nonnegative definite, special consideration is needed in those cases where $S^o(\omega)$ has a zero principal minor. For the discussion on this point, the reader is referred to Ref. [4].

Since the real and the imaginary parts of cross-spectral density functions are respectively even and odd in $\underline{\omega}$, it can be shown from successive substitutions using Eqs. 46 and 47 that

$$\text{Re } H_{jk}(\underline{\omega}) = \text{Re } H_{jk}(-\underline{\omega})$$

$$\text{Im } H_{jk}(\underline{\omega}) = -\text{Im } H_{jk}(-\underline{\omega})$$

(48)

for $j > k$, and

$$H_{jj}(\underline{\omega}) = H_{jj}(-\underline{\omega}) \geq 0$$

from which it follows that $h_{jk}(\underline{x})$ is real.

If $H_{jk}(\underline{\omega})$ is written in polar form;

$$H_{jk}(\underline{\omega}) = |H_{jk}(\underline{\omega})| e^{i\theta_{jk}(\underline{\omega})}$$

(49)

then, due to Eq. 48, the argument $\theta_{jk}(\underline{\omega})$ is anti-symmetric in $\underline{\omega}$, that is

$$\theta_{jk}(\underline{\omega}) = -\theta_{jk}(-\underline{\omega})$$

(50)

with $\theta_{jj}(\underline{\omega}) = 0$.

Once $H(\underline{\omega})$ is computed using Eqs. 46 and 47, then instead of passing a white noise vector through filters, the process $f_j(\underline{x})$ can be simulated in terms of the following series

$$f_j(\underline{x}) = \sum_{m=1}^{j} \sum_{\ell=1}^{N} |H_{jm}(\underline{\omega}_\ell)| \sqrt{2\Delta\underline{\omega}} \cos[\underline{\omega}_\ell \cdot \underline{x} + \theta_{jm}(\underline{\omega}_\ell) + \Phi_{m\ell}]$$

(51)

where $\underline{\omega}_\ell$, $\Delta\underline{\omega}$, N, and $\Phi_{m\ell}$ are essentially the same as defined previously for n-dimensional processes and

22

$$\theta_{jm}(\omega_\ell) = \tan^{-1}\left(\frac{\mathrm{Im}\, H_{jm}(\omega_\ell)}{\mathrm{Re}\, H_{jm}(\omega\ell)}\right) \tag{52}$$

It can be shown [4] that the processes $f_j(\underline{x})$ ($j = 1,\ldots,m$), as simulated by Eq. 51, possess the target cross-correlation functions and hence the target cross-spectral density, with respect to an ensemble average.

For digital simulation of sample functions of $f_j(\underline{x})$, Eq. 51 is used with $\Phi_{m\ell}$ being replaced by their realized values.

5. Simulation of Multidimensional Nonhomogeneous Processes

Simulations of nonstationary processes have been studied dealing mostly with earthquake ground motion. The common feature of these studies is that a nonstationary process is simulated by multiplying by an envelope function the stationary process generated either by filtering a white noise [13,14] or by a series of oscillations with random frequency and random phase [15,16,17].

The efficient method of simulation that has been proposed for multidimensional homogeneous processes can be directly generalized to a nonhomogeneous process characterized by an evolutionary power spectrum as introduced by Priestley [18,19].

It was seen from Eq. 9 that a homogeneous process is additively built up by orthogonal oscillations with random amplitudes. This concept of orthogonal components can be extended to that of the evolutionary process $f_e^o(x)$ expressed as

$$f_e^o(x) = \int_o^\infty B(x,\omega)[\cos \omega x dU(\omega) + \sin \omega x dV(\omega)] \qquad (53)$$

where $B(x,\omega)$ is a deterministic modulating function characterizing the "nonhomogeneity" of the process, and $U(\omega)$ and $V(\omega)$ are the same as defined in Eq. 10.

Using the orthogonal conditions of $U(\omega)$ and $V(\omega)$, the mean square of $f_e^o(x)$ is found to be

24

$$E[f_e^o(x)]^2 = \int_0^\infty B^2(x,\omega) S_1^o(\omega)\, d\omega = \int_0^\infty S_e^o(x,\omega)\, d\omega \qquad (54)$$

where $S_e^o(x,\omega) = B^2(x,\omega) S_1^o(\omega)$ is defined as the evolutionary power spectral density function.

For the detailed discussion and the estimation of the evolutionary power spectrum, the readers are referred to Refs. 18 and 19.

The direct generalization of the above discussion to n-dimensional process is obvious. Thus, if a real nonhomogeneous process has an evolutionary power spectral density function, the process $f_e^o(\underline{x})$ can be simulated by

$$f_e(\underline{x}) = \sqrt{2} \sum_{k=1}^N [B^2(\underline{x},\underline{\omega}_k) S(\underline{\omega}_k) \Delta\underline{\omega}]^{\frac{1}{2}} \cos(\underline{\omega}_k \cdot \underline{x} + \phi_k) \qquad (55)$$

where $B(\underline{x},\underline{\omega})$ is the n-dimensional modulating function and the remaining notations are the same as in the case of a homogeneous process given by Eq. 33. It can be shown that the simulated process $f_e(\underline{x})$ possesses the target evolutionary power spectrum as $N \rightarrow \infty$.

Note that in a particular case when $B(\underline{x},\underline{\omega}) = B(\underline{x})$, then $f_e^o(\underline{x})$ can be obtained by multiplying a homogeneous process simulated from $S_o(\underline{\omega})$ by the spatial envelope function $B(\underline{x})$.

A more detailed study with numerical examples on this method of simulation for nonhomogeneous Gaussian process with an evolutionary power spectral density has been made by Yang [6].

In the following section, the Gaussian nonhomogeneous
process with an evolutionary power spectral density is referred
to as Gaussian evolutionary process for simplicity.

6. Monte Carlo Solution of Structural Dynamics

The preceding method of digital generation of sample functions of a Gaussian process can be used for the Monte Carlo solution of the following structural problems. It is pointed out parenthetically that by adding a constant value m to the sample functions $\bar{f}(t,\underline{x})$ described in the preceding sections, one can generate sample functions of the simulated process $f(t,\underline{x}) + m$ associated with $f_0(t,\underline{x}) + m$. Note that the mean value of $f_0(t,\underline{x}) + m$ is no longer zero but it is equal to m.

(a) The method can be used in the response analysis of a nonlinear structure under random loading if such loading can be idealized as Gaussian homogeneous or Gaussian evolutionary process with constant mean values. In particular, if the modes $\mu_k(\underline{x})$ of the corresponding linear structures are known, the solution $y_0(t,\underline{x})$ is in approximation expanded into a finite series.

$$y_0(t,\underline{x}) = \sum_{k=1}^{K} q_k(t)\, \mu_k(\underline{x}) \tag{56}$$

When Eq. 56 is substituted into the governing (nonlinear partial) differential equation(s) of motion, one can usually get a set of simultaneous nonlinear but ordinary differential equations involving the generalized forces of the

27

following form;

$$F_k(t) = \int_D \mu_k(\underline{x}) \, f_o(t,\underline{x}) \, d\underline{x} \qquad (57)$$

where $f_o(t,\underline{x})$ is the random excitation process and D indicates an appropriate domain of integration. Sample functions $\bar{F}_k(t)$ can then be digitally generated from Equation 57 with $f_o(t,\underline{x})$ replaced by $\bar{f}(t;\underline{x})$;

$$\bar{F}_k(t) = \int_D \mu_k(\underline{x}) \, \bar{f}(t,\underline{x}) \, d\underline{x} \qquad (58)$$

It goes without saying that $\bar{f}(t,\underline{x}) + m$ has to be used in place of $\bar{f}(t,\underline{x})$ if the excitation process has a non-zero constant mean value since the simple superposition of solutions does not apply in this case because of nonlinearity.

The modes $\mu_k(\underline{x})$ often take the form of sinusoidal or hyperbolic functions or their combinations. Therefore, the integration in Eq. 58 can usually be carried out in closed form since $\bar{f}(t,\underline{x})$ is given as a sum of cosine functions. This is one of the significant advantages of the present method of simulation over other existing methods. In fact, if the domain of integration D represents a two or three dimensional space, the numerical integration of Eq. 58 will usually become an insurmountable obstacle. Another advantage is that the present method does not require the nonlinearity to be small or moderate, a condition

28

which has to be imposed for standard linearization or perturbation techniques.

Once the sample functions $\bar{F}_k(t)$ are evaluated from Eq. 58, then the sample functions $\bar{q}_k(t)$ of $q_k(t)$ can be numerically evaluated from the (simultaneous) nonlinear but ordinary differential equations mentioned above (replacing of course $F_k(t)$ by $\bar{F}_k(t)$ therein). The experience shows that this phase of numerical work is not a serious problem. Finally, the sample function $\bar{y}(t,\underline{x})$ of the solution $y_o(t,\underline{x})$ can be obtained from Eq. 56 with $q_k(t)$ replaced by $\bar{q}_k(t)$. The temporal average of $\bar{y}^2(t,\underline{x})$ over a sufficiently long period of time will produce the mean square response in the Monte Carlo sense if the processes involved are ergodic. Otherwise, the ensemble average has to be considered.

Reference [20] represents a typical example of such analysis. A segment of a sample function of the tip deflection $U(0,t)$ of a vertical pile of uniform cross-section in deep water (Fig. 6) having nonlinear drag effect and subjected to unidirectional wind-induced waves is shown in Fig. 7, where a segment of a sample function of the response of the corresponding linear pile (without drag term) is also shown for comparison. In this study, the excitation is due to waves under fully developed sea conditions with

29

mean wind velocity V for which the Pierson - Moskowitz spectrum $S_1^o(\omega)$ for the ocean-surface elevation has been used;

$$S_1^o(\omega) = \frac{\alpha g^2}{\omega^5} \, e^{-\beta(\omega_o/\omega)^4} \qquad (59)$$

where $\alpha = 8.10 \times 10^{-3}$, $\beta = 0.74$ and $\omega_o = g/V$ with g = acceleration due to gravity and V = mean wind velocity.

The application of this type of Monte Carlo approach has also been made to other nonlinear structural response analysis [3,4,21,22,23].

(b) The method can be applied to the failure analysis of a structure with spatially random variation of strength and other material properties. In this case, sample structures are generated by digitally generating such spatial variations of strength and other material properties. When correlated spatial variations are observed on more than one material property (e.g. Young's modulus and density), usually a multidimensional multivariate process has to be generated with the aid of the method described in Section 4.

Applying to each of these sample structures a sample stress history of a random stress process, the fatigue life of a sample structure can be computed under the

assumption of a certain fatigue failure mechanism. The
statistical variation of the fatigue life thus computed
establishes its empirical distribution under the random
stress process in the Monte Carlo sense. This approach
was successfully taken in Ref. [24]. A similar problem in
which the empirical distribution of the static failure
load is to be found for a concrete structure with spatial
strength variation is treated in detail in Ref. [25].

(c) The method can be employed effectively when the
structural system to be analyized is complex even though
it involves neither nonlinearity nor random variation of
material properties. The mean square responses (displace-
ment, shear force and bending moment) of a large floating
plate to wind-induced random ocean-waves are computed in
Ref. [26] taking the temporal averages of sample response
functions as in Ref. [20]. The analysis is essentially
numerical since sample functions of the wind-induced ocean-
surface elevation are digitally generated and the corres-
ponding response functions are numerically obtained. This
was done because the ocean-structure system considered was
too complex to solve analytically. Another example of this
kind is the study of the dynamic interaction between moving
vehicles and a bridge with random pavement surface rough-

ness [27]. In this problem the random pavement surface

roughness is digitally simulated for numerical response

analysis.

In some problems of mechanics, a structure is considered

complex when its material properties are spatially random.

The wave propagation through a random medium is one of these

problems. In Ref. [28], the stress wave propagation through

a finite cylinder with random material properties is treated

under the condition that the one end of the cylinder is acted

upon by an impact load and the other end is free. A set

of one hundred samples of correlated random material properties

(Young's modulus and density) are generated thus producing

one hundred sample cylinders. The finite element method is

applied for the stress analysis to compute maximum stress

intensity in each of these cylinders due to the impact. An

empirical distribution of the maximum stress intensity is

then established in the Monte Carlo sense.

(d) Finally, the method is often useful when the

problem is to determine eigenvalues (frequencies and buckling

loads) of the structure with random material properties. As

in the case of the wave propagation problems, sample struc-

tures are generated and the statistical distribution of

eigenvalues of these structures are treated as the empir-

ical distribution of the eigenvalue of interest. An

example of this problem is given in Ref. [29].

REFERENCES

[1]   Rice, S. O., "Mathematical Analysis of Random Noise" in

"Selected Papers on Noise and Stochastic Processes" edited

by N. Wax, Dover Publications, Inc., New York, 1954,

pp. 180 - 181.

[2]   Borgman, L. E., "Ocean Wave Simulation for Engineering

Design", J. of Waterways and Harbors Div., Proc. ASCE,

Vol. No. WW 4, Nov. 1969, pp. 556 - 583.

[3]   Shinozuka, M. "Simulation of Multivariate and Multidimen-

sional Random Processes", J. of Acoustical Soc. of Am.,

Vol. 49, No. 1, Jan. 1971, pp. 357 - 367.

[4]   Shinozuka, M., and Jan, C.-M., "Simulation of Multivariate

and Multidimensional Random Processes II", NSF-GK 3858/

24925, Technical Report No. 12, Department of Civil

Engineering and Engineering Mechanics, Columbia University,

April 1971, submitted for publication in the Journal of

Acoustical Society of America.

[5]   Pugachev, V. S., "Theory of Random Functions", translation

by Blunn, O.M., Pergamon Press, Addison-Wesley Publishing

Company, Inc., Reading, Mass., Palo Alto, London, 1965,

pp. 228 - 232.

[6] Yang, J.-N., "Simulation of Random Envelope Processes",

private communication, to appear in Journal of Sound and

Vibration.

[7] Cramér, H. and Leadbetter, M. F., "Stationary and Related

Stochastic Processes", John Wiley, New York, 1967, p. 249.

[8] Lyon, R. H., "Statistics of Combined Sine Waves", Journal

of Acoustical Society of America, Volume 48, No. 1 (Part 2),

January 1970, pp. 145 - 149.

[9] Bochner, S., "Lectures on Fourier Integrals", English trans-

lation by M. Tenebaum and H. Pollard, Annals of Mathematic

Studies No. 42, Princeton University Press, Princeton,

New Jersey, 1959, pp. 325 - 328.

[10] Cramér, H. and Leadbetter, M. F., ibid., p. 161 and p. 135.

[11] Eby, E. S., "Synthesis of Multivariate Gaussian Random

Processes with a Preassigned Covariance", IEEE Transactions

of Information Theory, November 1970, pp. 773 - 776.

[12] GantMacher, F. R., "The Theory of Matrices", Vol. 1, Chelsea,

New York, 1960, p. 37.

[13] Shinozuka, M. and Sato,Y., "Simulation of Nonstationary

Random Processes", Proc. ASCE, 93, EM 1, 1967, pp. 11 - 40.

[14] Amin, M. and Ang, A. H.-S., "Nonstationary Stochastic Models

of Earthquake Motions", EMD Journal, ASCE, Vol. 94, No. Em 2,

April 1968, pp. 559 - 583.

[15] Goldberg, J. E., Bogdanoff, J. L. and Sharpe, D. R., "The

Response of Simple Nonlinear Structure to a Random Dis-

turbance of Earthquake Type", Bull. Seis. Soc. Am., Vol. 54,

No. 1, 1964, pp. 263 - 276.

[16] Goto, H. and Toki, K., "Structural Response to Nonstationary

Random Excitation", 4th WCEE, Santiago, 1969.

[17] Shinozuka, M. and Brant, P. W., "Application of Evolutionary

Power Spectrum in Structural Dynamics", Tech. Rpt. No. 3,

NSF-GK 3858, Columbia University, 1969.

[18] Priestly, M. B., "Evolutionary Spectra and Nonstationary

Processes", J. R. Stat. Soc., B 27, 1965, pp. 204 - 236.

[19] Priestley, M. B., "Power Spectral Analysis of Nonstationary

Random Processes", J. Sound Vibr. 6, 1967, pp. 86 - 97.

[20]   Shinozuka, M., and Wen, Y.-K., "Nonlinear Dynamic Analysis

of Offshore Structures; A Monte Carlo Carlo Approach"

in "Stochastic Hydraulics" (Proceedings of the First

International Symposium on Stochastic Hydraulics),

University of Pittsburgh Press, pp. 507 - 521.

[21]   Shinozuka, M. and Wen, Y.-K., "Monte Carlo Solution of

Nonlinear Vibration", AIAA Journal, Vol. 10, No. 1,

January 1972, pp. 39 - 40.

[22]   Wen, Y.-K., and Shinozuka, M., "Monte Carlo Solution of

Structural Response to Wind Load", Proceedings of the

3rd International Conference on Wind Effects on Buildings

and Structures, Tokyo, Japan, September 6 - 11, 1971,

Part III, pp. IIL 3 - 1 - IIL 3 - 8.

[23]   Vaicaitis, R. and Jan, C.-M., and Shinozuka, M., "Non-

linear Panel Response and Noise Transmission from a

Turbulent Boundary Layer by a Monte Carlo Approach",

NSF GK 3858 and GK 24925, Technical Report No. 13,

Columbia University, 1971, AIAA Paper No. 72 - 199, AIAA

10th Aerospace Sciences Meeting, San Diego, California,

January 17 - 19, 1972.

[24] Itagaki, H. and Shinozuka, M., "Applications of Monte Carlo Technique to Fatigue Failure Analysis under Random Loading", NSF GK 3858/24925, Technical Report No. 16, Department of Civil Engineering and Engineering Mechanics, Columbia University, June 1971, to be published in a special technical publication of ASTM.

[25] Shinozuka, M., "Probabilistic Formulation for Analytical Modeling of Concrete Structures", Technical Report CR 72.005, Naval Civil Engineering Laboratory, Port Hueneme, California, Sponsored by Naval Facilities Engineering Command, under Contract N62399-71-C-0022, November, 1971.

[26] Wen, Y.-K. and Shinozuka, M., "Response of a Large Floating Plate to Ocean Waves", NSF GK 3858/24925, Technical Report No. 14, Department of Civil Engineering and Engineering Mechanics, Columbia University, June 1971, accepted for publication in the Journal of Waterways and Harbors Div., ASCE.

[27] Shinozuka, M. and Kobori, T., "Fatigue Analysis of Highway Bridges", NSF GK 3858 Technical Report No. 8, Department of Civil Engineering and Engineering Mechanics, Columbia University, January 1971, presented at the
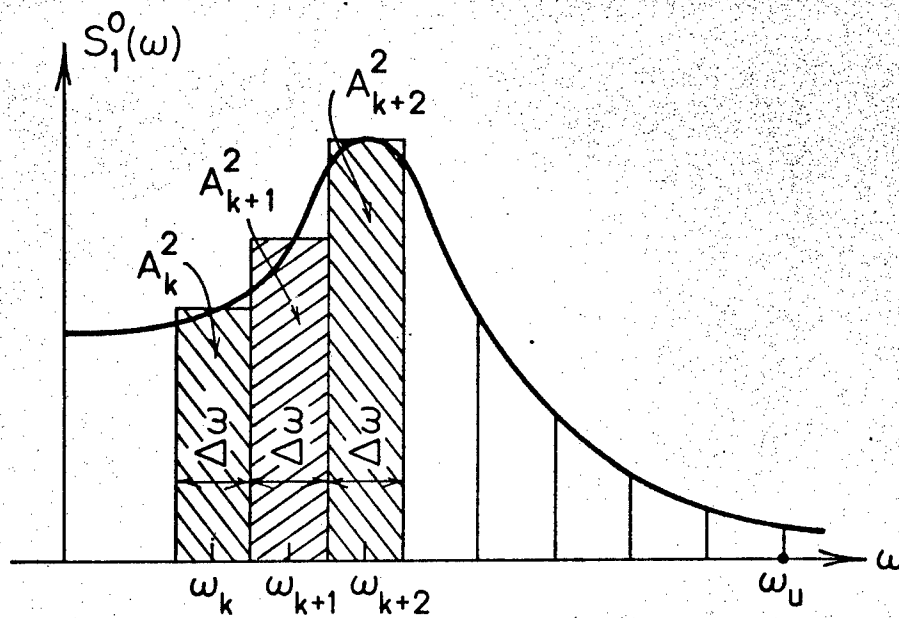
ASCE National Meeting on Structural Engineering in

Baltimore, April 19 - 23, 1971.

[28]   Astill, J. C., Nosseir, B. and Shinozuka, M., "Impact

Loading on Structures with Random Properties", to be

published in the Journal Structural Mechanics, Vol. 1,

No. 1, 1972.

[29]   Shinozuka, M. and Astill, C. J., "Random Eigenvalue

Problems in Structural Mechanics", AIAA Paper No. 71 - 149,

AIAA 9th Aerospace Sciences Meeting, New York, New York,

January 1971, to appear in the American Institute of

Aeronautics and Astronautics Journal.

LIST OF FIGURES

$$\bar{f}(x) = \sqrt{2} \sum_{k=1}^{N} A_k \cos(\omega_k x + \phi_k)$$

where $A_k \doteq \sqrt{S_1^0(\omega_k)\Delta\omega}$

$$\omega_k = (k - \tfrac{1}{2})\Delta\omega$$

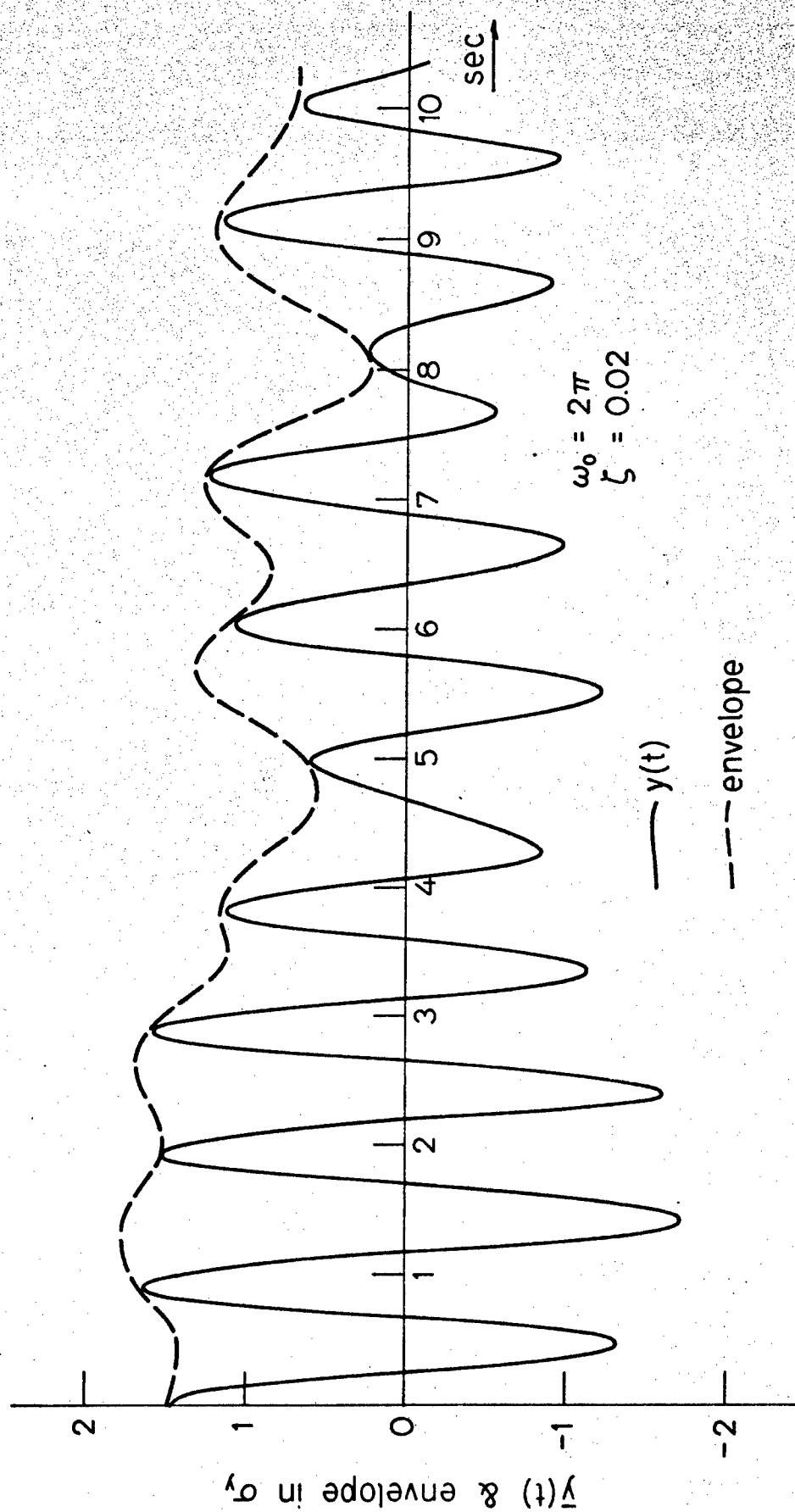$$\omega_u = N\Delta\omega$$

Fig. 1 One-sided spectral density

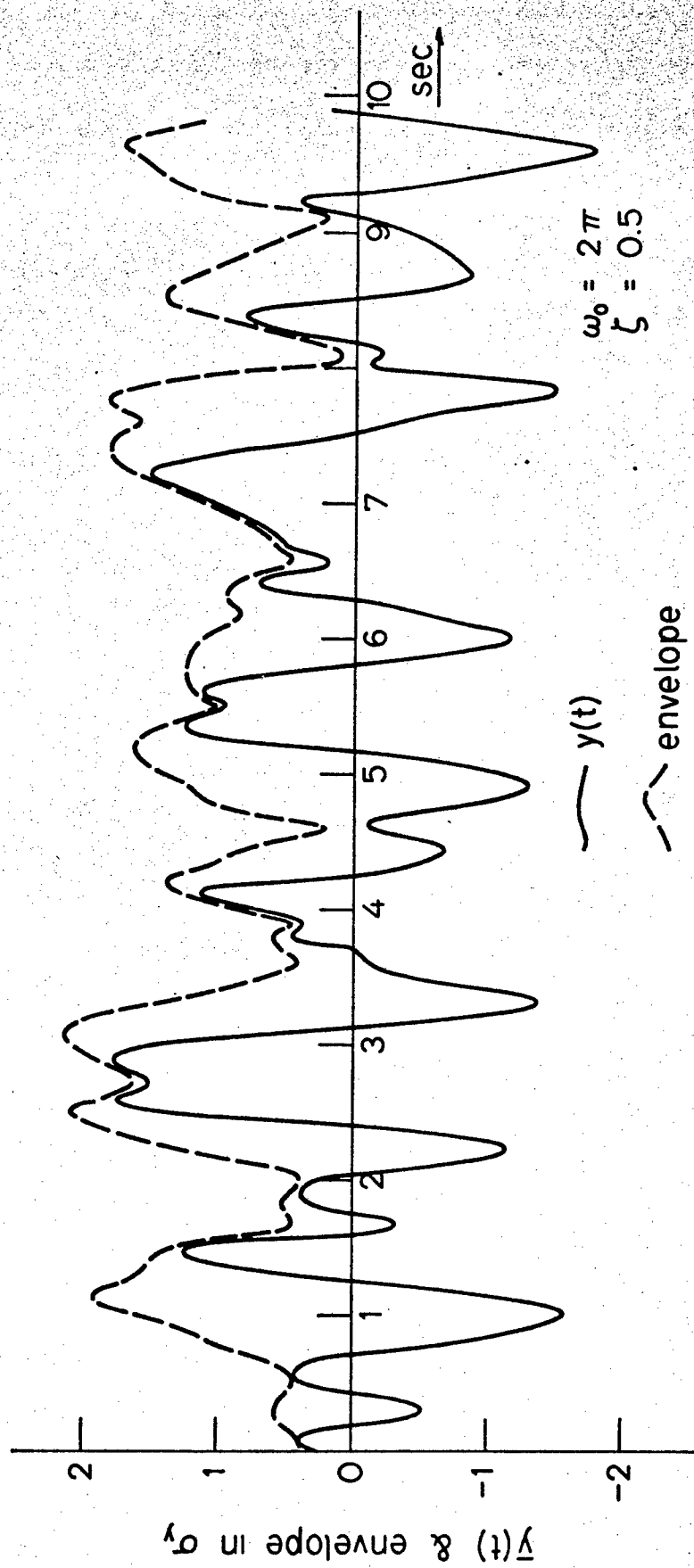Fig. 2 Sample functions of a narrow-band random process

and its envelope process

$\omega_0 = 2\pi$
$\zeta = 0.02$

—— y(t)

--- envelope

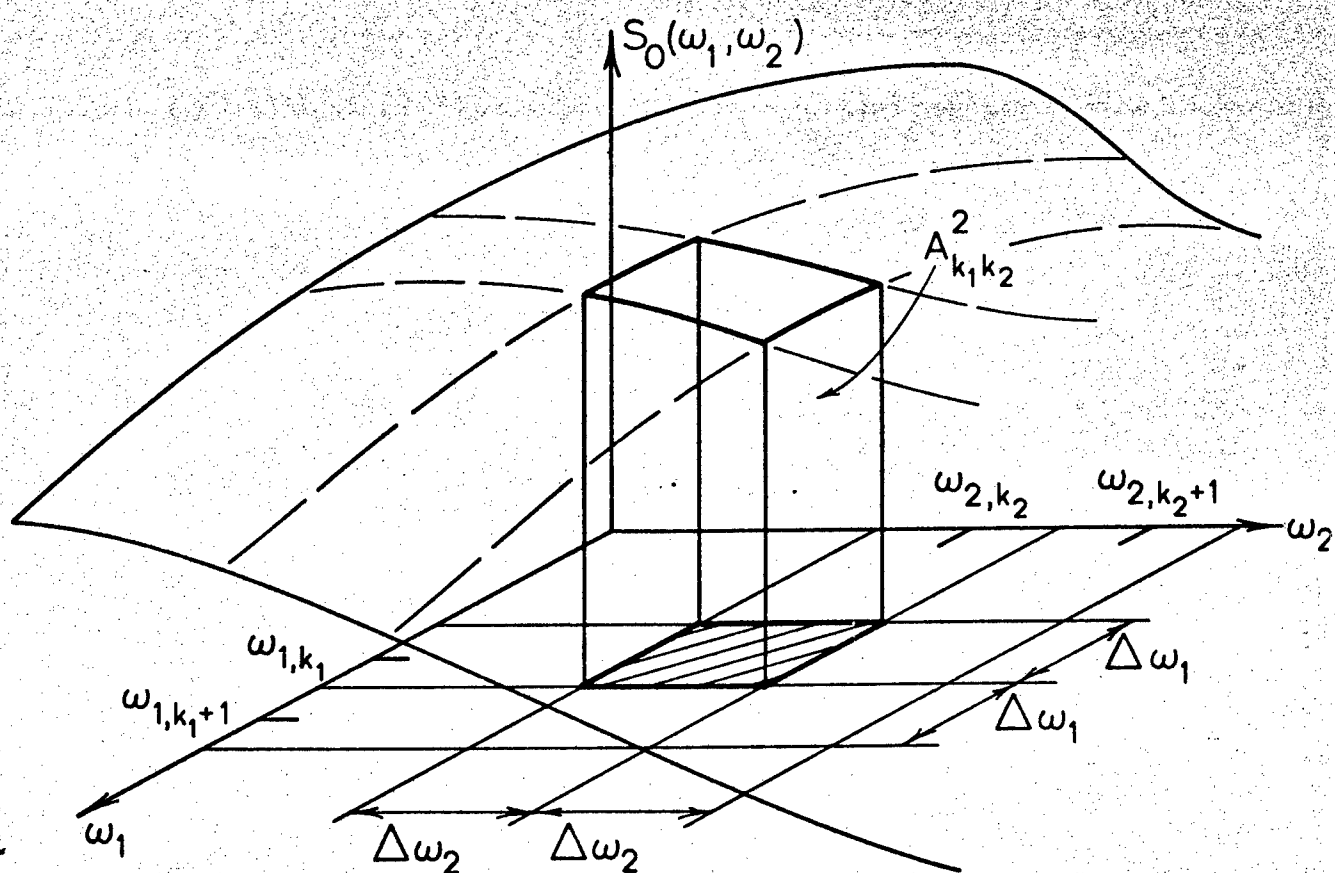y(t) & envelope in σ_y

Fig. 3   Sample Functions of a wide-band random process

and its envelope process

$$\bar{f}(x_1, x_2) = \sqrt{2} \sum_{k_1=1}^{N_1} \sum_{k_2=1}^{N_2} A_{k_1 k_2} \cos(\omega_{1k_1} x_1 + \omega_{2 k_2} x_2 + \phi_{k_1 k_2})$$

where $\quad A_{k_1 k_2} \doteq \sqrt{S_0(\omega_{1k_1}, \omega_{2k_2}) \, \Delta\omega_1 \, \Delta\omega_2}$

$$\omega_{1k_1} = (k_1 - \tfrac{1}{2}) \Delta\omega_1 , \quad \omega_{2k_2} = (k_2 - \tfrac{1}{2}) \Delta\omega_2$$

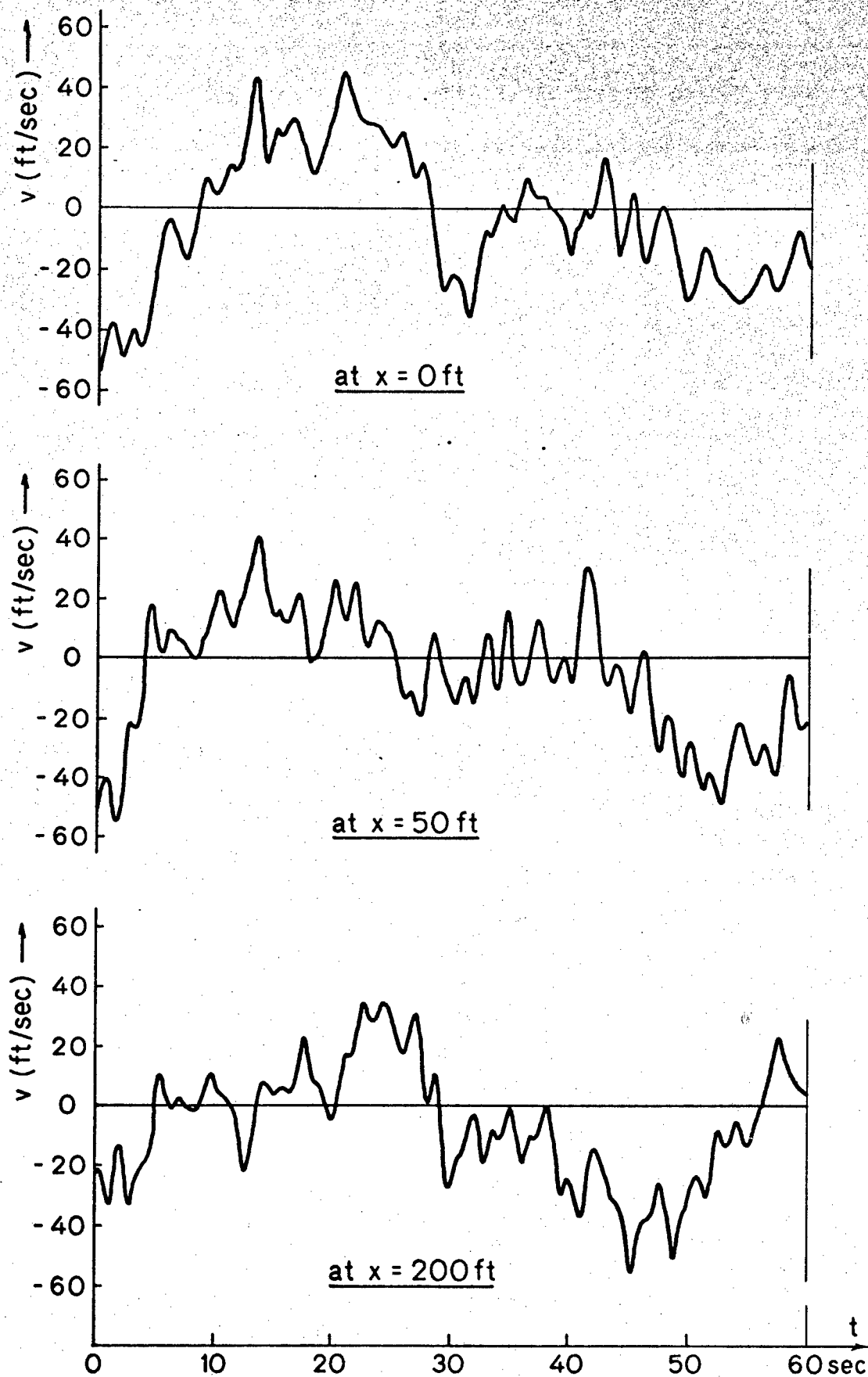Fig. 4 Two-dimensional spectral density
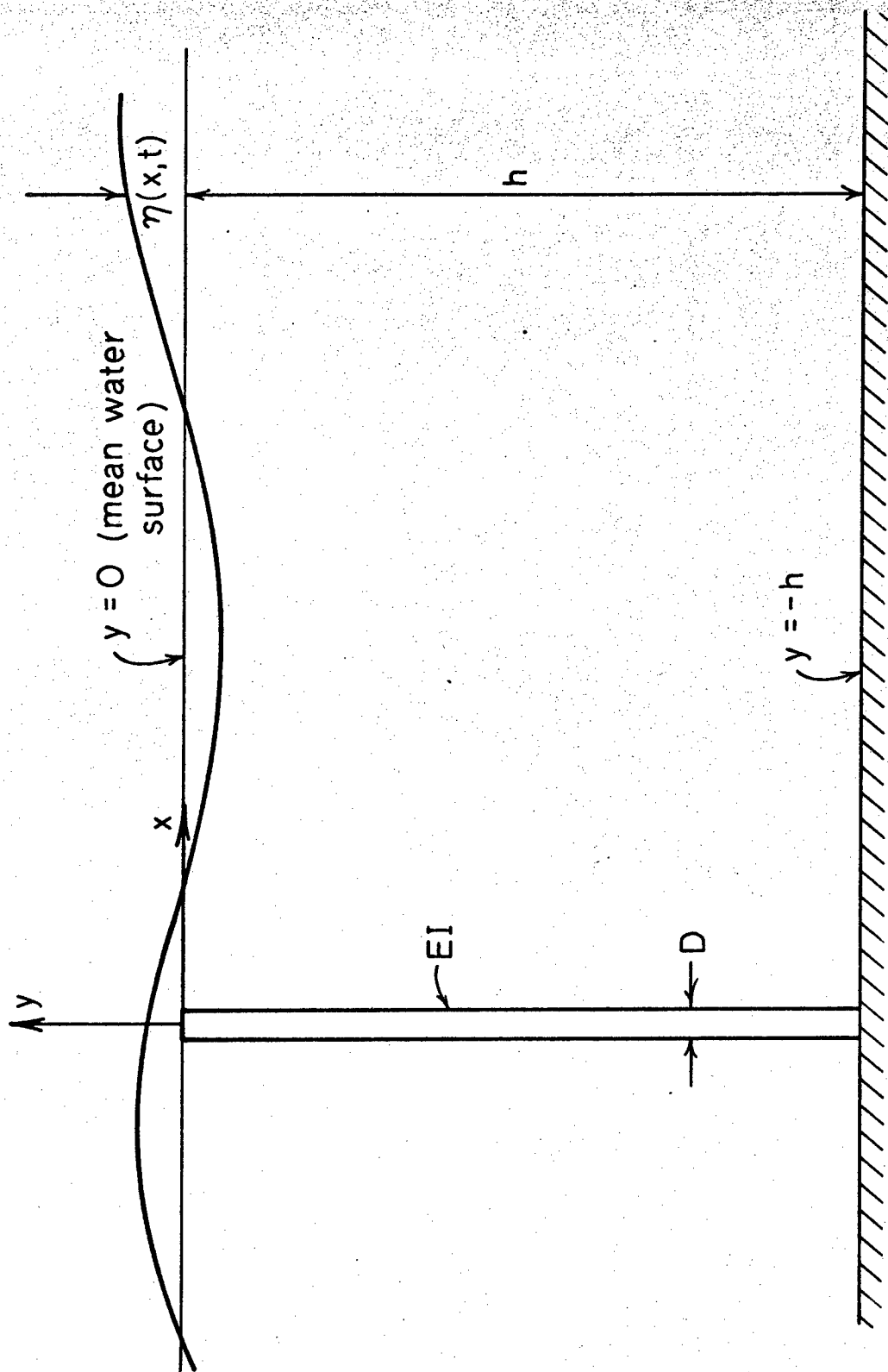
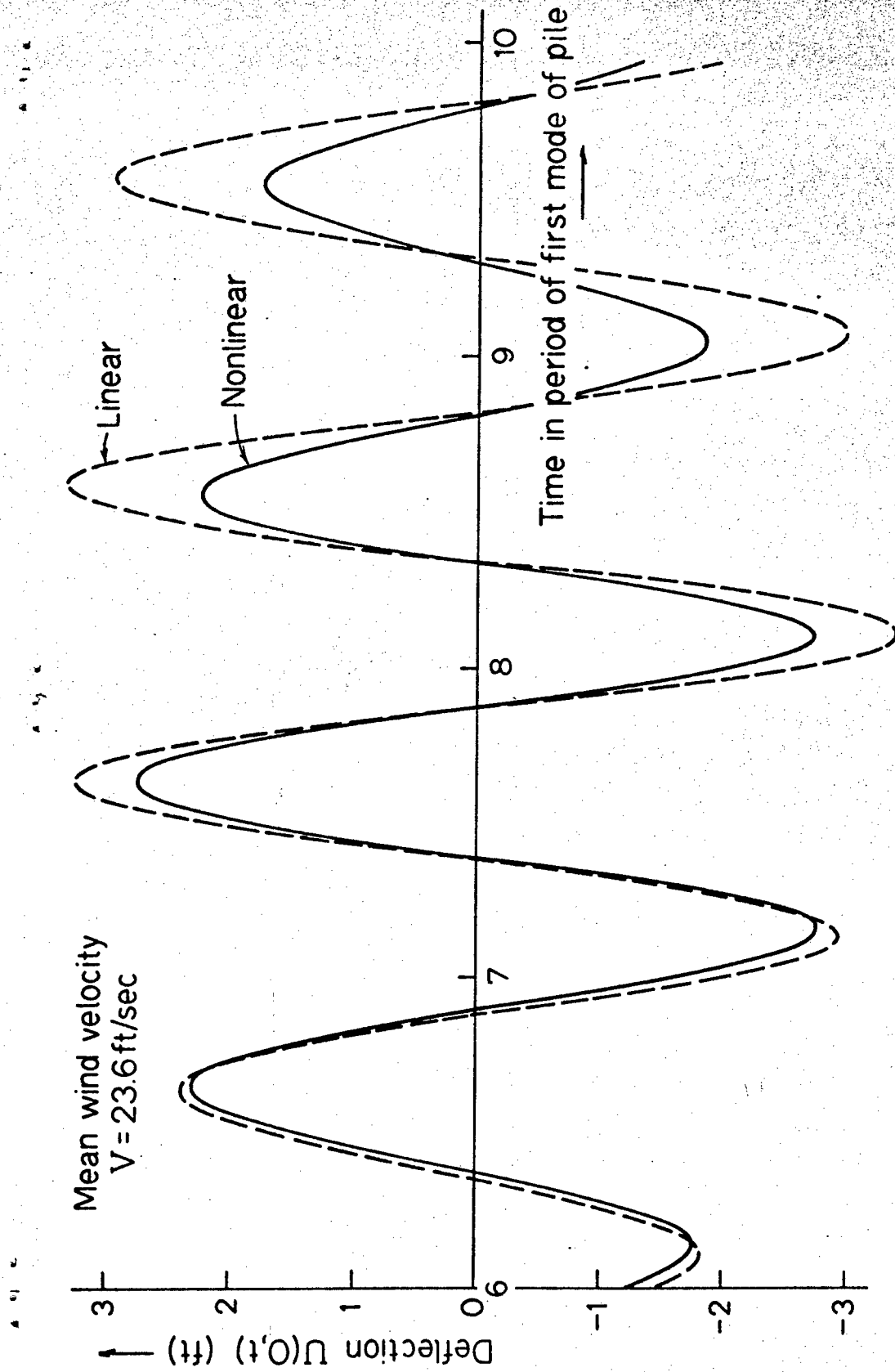Fig. 5 Simulation of wind velocity at different points

Fig. 6 Ocean – pile system

Fig. 7 A section of sample response function at mean wind velocity 23.6 ft/sec

DOCUMENT CONTROL DATA - R & D

(Security classification of title, body of abstract and indexing annotation must be entered when the overall report is classified)

1. ORIGINATING ACTIVITY (Corporate author)	2a. REPORT SECURITY CLASSIFICATION
Columbia University	Unclassified
	2b. GROUP

3. REPORT TITLE

Monte Carlo Solution of Structural Dynamics

4. DESCRIPTIVE NOTES *(Type of report and inclusive dates)*

Technical Report

5. AUTHOR(S) *(First name, middle initial, last name)*

M. Shinozuka

6. REPORT DATE	7a. TOTAL NO. OF PAGES	7b. NO. OF REFS
March 27 - 29, 1972	48	29

8a. CONTRACT OR GRANT NO.	9a. ORIGINATOR'S REPORT NUMBER(S)
National Science Foundation	NSF GK 24925
b. PROJECT NO.	
Grant GK 24925	Technical Report No. 19
c.	9b. OTHER REPORT NO(S) *(Any other numbers that may be assigned this report)*
d.	

10. DISTRIBUTION STATEMENT

Distribution is unlimited

11. SUPPLEMENTARY NOTES	12. SPONSORING MILITARY ACTIVITY
	None

13. ABSTRACT

In spite of the recent remarkable advance in the area of stochastic mechanics, the present state of art still leaves a number of difficulties unsolved that must be overcome before the approach becomes more useful. Such problem areas include (1) random response analysis of highly non-linear structures, (2) failure analysis of structures under random loading, (3) analysis of extremely complex systems and, (4) random eigenvalue problems.

The recent advent of high speed digital computers, however, has made it not only possible but also highly practical to apply the Monte Carlo techniques to a large variety of engineering problems. The present paper presents a technique of digital simulation of multivariate and/or multidimensional Gaussian random processes (homogeneous or nonhomogeneous) which can represent physical processes germane to structural engineering. The paper also describes a method of digital simulation of envelope functions. Such simulations are accomplished in terms of a sum of cosine functions with random phase angles and used as the basic tool in a general Monte Carlo method of solution to a wide class of problems in structural engineering, particularly those mentioned above.

DD FORM 1473 (PAGE 1)
1 NOV 65

S/N 0101-807-6801

KEY WORDS	LINK A		LINK B		LINK C	
	ROLE	WT	ROLE	WT	ROLE	WT
Monte Carlo Techniques						
Simulation of Multivariate and/or Multidimensional Random Processes						
Stochastic Mechanics						
F F T						
Nonstationary or Nonhomogeneous Stochastic Processes						
Random Vibration						
Envelope Processes						